Can. J. Remote Sensing, Vol. 36, Suppl. 2, pp. S257–S265, 2010

Research note / Note de recherche

Mapping changing temperature patterns over a glacial moraine using oblique thermal imagery and lidar

C. Hopkinson, J. Barlow, M. Demuth, and J. Pomeroy

Abstract. Due to access difficulties in active alpine moraine environments, it can be challenging to accurately map and quantify debris cover and ice-core extent. To aid in identifying the presence and extent of ice-cored moraine, a non-invasive method of mapping spatial and temporal moraine temperature patterns using a light detection and ranging (lidar) digital elevation model (DEM) and sequences of oblique thermal imagery was evaluated. A procedure of lidar DEM-based orthorectification of thermal images collected through time from different locations enabled maps of temperature change to be generated and thermal signatures plotted. Although no exposed ice was visible on the moraine slope studied, the presence of shallow ice core beneath the debris-covered surface was inferred in areas of cooler temperatures during daylight solar heating and rapid thermal decay after sunset. It is presumed that this apparent increased heat loss in some areas of the moraine is being used to drive internal melt processes. It is believed that such temporal thermal imaging at high repetition frequency will aid in remotely mapping the presence of buried ice and, with the combination of energy balance data and further field validation, could enable the estimation of debris cover depth.

Résumé. En raison des difficultés d'accès dans les environnements de moraines alpines actives, il peut être difficile de cartographier et de quantifier de façon précise le couvert de débris et l'étendue du noyau de glace. Afin de faciliter l'identification de la présence et de l'étendue des moraines à noyau de glace, on a évalué une méthode non invasive de cartographie des patrons spatiaux et temporels des températures de moraines à l'aide d'un MNE dérivé des données lidar et des séquences d'images thermiques en oblique. Une procédure d'orthorectification basée sur un MNE dérivé des données lidar d'images thermiques acquises dans le temps à partir de différentes localisations a permis de générer des cartes de changements des températures et de tracer des signatures thermiques. Bien qu'aucune glace exposée n'ait été visible sur le versant de moraine étudié, la présence de noyaux de glace peu profonds sous la surface recouverte de débris a pu être déduite dans les zones de températures plus froides durant la période de réchauffement solaire diurne et de décroissance thermique rapide après le coucher du soleil. On présume que cette perte de chaleur apparente accrue dans certaines zones de la moraine sert à conduire les processus de fonte interne. On croit que de telles images thermiques temporelles à des fréquences de répétition élevées faciliteront la cartographie par télédétection de la présence de glace enfouie et, en combinaison avec les données du bilan d'énergie et de validation additionnelle sur le terrain, pourraient permettre d'estimer l'épaisseur du couvert de débris.
[Traduit par la Rédaction]

Introduction

Glaciers in western Canada play an important role both as indices of climatic change (Demuth et al., 2008) and in terms of regulating long-term runoff regimes (Young, 1991). This second ‘‘reservoir-like’’ attribute of generally storing water as snow and ice during years of otherwise high runoff and releasing it is as melt during drought years has meant that downstream users have been able to build communities and develop hydro-power, irrigation, manufacturing, and resource-extraction activities based on the expectation of reliable river flow regimes. However, development within downstream areas over the last century has taken place during a period of steady glacier recession. Consequently, the flow-regulation attributes of glaciers in some regions are diminishing, and it has already been shown that the often-presumed reservoir-like

Received 10 October 2009. Accepted 28 November 2009. Published on the Web at http://pubservices.nrc-cnrc.ca/cjrs on 21 January 2011.

C. Hopkinson.[1] Applied Geomatics Research Group, Annapolis Valley Campus, Centre of Geographic Sciences (COGS), Lawrencetown, NS B0S 1M0, Canada.

J. Barlow. Department of Geography, Durham University, Durham DH1 3LE, UK.

M. Demuth. Geological Survey of Canada, Natural Resources Canada, 601 Booth Street, Ottawa, ON K1A 0E8, Canada.

J. Pomeroy. Department of Geography, University of Saskatchewan, Saskatoon, SK S7N 5A5, Canada.

[1]Corresponding author (e-mail: Chris.hopkinson@nscc.ca).

behaviour of glaciers does not always hold during periods of rapid recession (Hopkinson and Young, 1998; Stahl et al., 2008; Comeau et al., 2009). As glacier extents recede, the proportional contribution of other hydrological sources within these basins increases. One source of meltwater production that has received limited attention is that of buried ice or ice-cored moraine in the periglacial environment (Østrem, 1959); as "white" ice extents diminish, the areas of ice-cored lateral moraine grow and provide a relatively small but steady supply of meltwater to basin runoff. For example, in a study of the processes contributing to moraine downwasting over the Kötlujökull Glacier in Iceland, Krüger and Kjær (2000) estimated that approximately 35% or 0.5 m of the total annual surface lowering was due to melting of internal ice.

Although many field-monitoring and research campaigns are ongoing in the mountains of western Canada to study glacial and periglacial volumetric variations, no glacier sites in Canada have implemented long-term systematic remote sensing based monitoring. This research note reports on tests to develop an in situ remote monitoring method aimed at mapping thermal signatures over lateral moraine areas for the purpose of better understanding shallow ice-core distributions and melt dynamics of these systems. The method of generating diurnal thermal orthomaps from oblique images collected over the lateral moraines on the north side of Peyto Glacier is presented and preliminary results are discussed.

The study was carried out at Peyto Glacier (51°40′N, 116°35′W) in the Canadian Rocky Mountain headwaters of the Mistaya River (**Figure 1**), which ultimately drains into the North Saskatchewan River and Nelson River basins. Peyto Glacier currently hosts a glaciological research and monitoring station and has been extensively studied since 1966 when it was chosen for inclusion as a reference site for the International Hydrological Decade (Munro, 2006). The glacier remains a focal point for much glacial hydrological and remote sensing research activity (Demuth and Pietroniro, 1999; Hopkinson and Demuth, 2006; Demuth et al., 2006; 2008).

Peyto Glacier ranges in altitude from approximately 2100 to 3150 m above sea level (asl), covers approximately 11 km^2, and has undergone significant terminus recession (approx. 1 km) and a long-term negative mass balance since the start of formal observations in 1966 (Demuth and Keller, 2006). The ablation zone lies within a narrow valley surrounded by steep mountain slopes. Convergent glacial ice streams flow northeasterly over a band of resistant dolostone below the long-term equilibrium line. Approximately 20% of the ablation zone is now debris covered. Medial moraines running down the length of the glacier ablation zone protrude above the surrounding ice surface by up to nearly 10 m in places due to differential debris cover and rates of melt. Lateral moraines surrounding the glacier terminus area have previously been reported or suspected to contain ice core (Østrem and Arnold, 1970; Nakawo and Young, 1982; Johnson and Power, 1985). Contemporary field observations of landslide scars demonstrate that the steep lateral moraines on the south side of Peyto Glacier possess a large volume of internal ice core, whereas the less steep moraine slopes on the north side do not reveal any such surficial ice exposures. However, four light detection and ranging (lidar) surveys collected in 2000, 2002, 2006, and 2007 (Hopkinson et al, 2001; Hopkinson and Demuth, 2006) have demonstrated that both lateral moraines surrounding the terminus region are highly mobile, with vertical downwasting of approximately 1 m/year and migration of the moraine crests toward the glacier margin of up to 6 m/year (Hopkinson et al., 2009). Two mechanisms were suggested by Hopkinson and Demuth (2006) for this rapid rate of moraine downwasting and motion: (*i*) gravitational slumping of the moraine due to debutressing at the

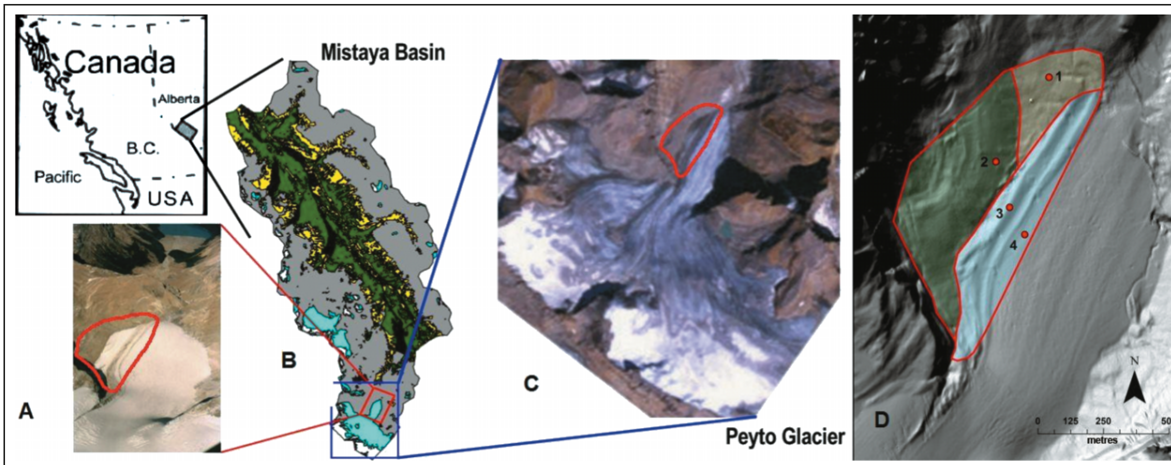

Figure 1. Study area. (A) Oblique aerial photograph of Peyto Glacier ablation zone and lateral moraine. (B) Mistaya Basin land covers (grey denotes bedrock, till, and talus; green denotes forest; yellow denotes meadow; blue and white denote glacier). (C) Landsat thematic mapper (TM) false colour composite of Peyto Glacier. (D) Lidar shaded relief illustrating glacial land surfaces of interest (1, relatively stable lateral moraine; 2, actively mobile lateral moraine; 3, medial moraine; 4, exposed glacial ice).

foot of the slope as the glacial ice melts downwards and away from the slope; and (*ii*) loss of volume (deflation) due to melting of internal ice. Field observations of glacier margin recession in concert with meltwater drainage from lateral moraines clearly indicate that both processes are active on the Peyto Glacier lateral moraines. However, the relative contribution of each process to the observed volumetric loss and high mobility is not known. Therefore, practical methods that can be implemented within the scope of existing mass balance and annual glacial monitoring visits need to be developed to assist with such quantifications.

Traditional methods to detect and map ice core within a moraine can be invasive (e.g., drilling) and laborious (e.g., ground-penetrating radar). Thermal imaging of moraines to remotely detect the presence of ice buried beneath a thin mantle of debris cover has obvious advantages over time-consuming point- and transect-based field observations. However, satellite (e.g., Landsat and Advanced Spaceborne Thermal Emission and Reflection Radiometer (ASTER)) or airborne thermal infrared (TIR) imaging is limited in terms of pixel resolution, temporal availability, and (or) acquisition cost (Kääb, 2008). The use of a field thermal imaging camera has the advantage of proximity to the subject (hence good pixel resolution) and the flexibility for rapid deployment multiple times during periods of changing thermal conditions (e.g., Pomeroy et al., 2009). However, field-collected images have limited spatial coverage and are oblique, and image sequences are needed during heating and cooling stages to have any chance of detecting the influence of buried ice on moraine surface temperatures. Thus, the purpose of this research note is to evaluate a method of TIR image acquisition, orthorectification, mosaicing, and temperature signature generation for the purpose of ice-cored moraine investigation. Preliminary results are illustrated and discussed, and a more thorough investigation into the actual location of ice-cored moraines and debris cover depths will be the focus of a follow-up study.

Data collection and analysis

Digital elevation model

A high-resolution digital elevation model (DEM) was needed to enable orthorectification of the oblique TIR imagery. A joint airborne and terrestrial lidar data collection campaign was performed during the first week of August 2007. Only the airborne lidar has been used in the presented analysis, as the terrestrial lidar was susceptible to occlusion over the heterogeneous terrain of the glacial moraines, and the resultant point cloud had many data voids. Several pieces of information are needed to compute the location of a laser pulse return from an aircraft, namely the position and orientation of the aircraft, laser pulse round-trip travel time, scan angle, and the speed of light. The raw lidar point data were gridded to regular raster arrays at a resolution of 1 m using an inverse distance weighted algorithm in Surfer software (Golden Software, Golden, Colo.). The lidar data were directly registered to a first-order North American Datum for 1983 Canadian Spatial Reference System (NAD83-CSRS) monument on the Icefields Parkway using a differential global positioning system (GPS). A description of the lidar data collection and processing methods is given in Hopkinson and Demuth (2006) and Hopkinson et al. (2009).

Diurnal thermal signatures

Oblique thermal images were collected over the lateral moraine area on the north side of Peyto Glacier (**Figure 1D**) on 1 August 2007, a calm clear sky day during the same week as that of the airborne lidar mission. The theory is that the spatial pattern of both temperature rise and decay will be modified as a result of heat loss to a melting ice surface beneath the moraines (Lougeay, 1974; 1982), i.e., in the case of daytime solar heating of the moraine surfaces, if heat is being lost to debris-covered ice core in the form of latent heat, the observed temperature rise will be reduced relative to that of a similar surface with similar heat inputs but no ice core. Conversely, nighttime cooling in ice-cored areas should prove to be more rapid than non-ice-cored areas due to the sensible heat stored in the debris cover being scavenged to drive melt or raise the temperature of ice toward the melting point. A preliminary test of this theory was conducted by collecting four sets of diurnal thermal imagery (48 images total) during clear sky radiation conditions using a tripod-mounted ThermaCam forward looking infrared, professional series (FLIR P) camera (**Figure 2**). The manufacturer-quoted specifications of the camera are as follows: field of view $24^\circ \times 18^\circ/0.3$ m, spatial resolution 1.3 mrad, thermal sensitivity 0.08 °C, electronic zoom $2\times$–$4\times$, 320×240 pixel array, 32 bit image resolution, spectral range 7.5–13.0 µm, and accuracy $\pm 2\,^\circ$C or 2% of the observed temperature range.

Images were collected at four photo-stations at a constant height of 1.7 m above the ground surface. Surface emissivity was set at 98% for all image acquisitions, and the air temperature within the scene was varied based on real-time temperature readings at the nearby Peyto Glacier research hut. Between two and four images were collected at each station at each time interval with sufficient sidelap (at least 25%) to cover the entire area of interest and ensure that the images could be aligned with each other in postprocessing. Each acquisition period took approximately 30 min to visit all four sites, and the approximate observation times were 10:30, 16:30, 20:30, and 22:00 (note that daytime collection frequency was limited due to other ongoing experiments on the glacial ice). The four photo-stations (**Figure 2**) were located on stable ground at the northeastern end of the lateral moraine, each offering a slightly different vantage point over the moraine surface, with the easternmost station being the lowest in elevation and the westernmost station lying almost 100 m higher. The photo-stations were surveyed using rapid static differential GPS techniques and were differentially

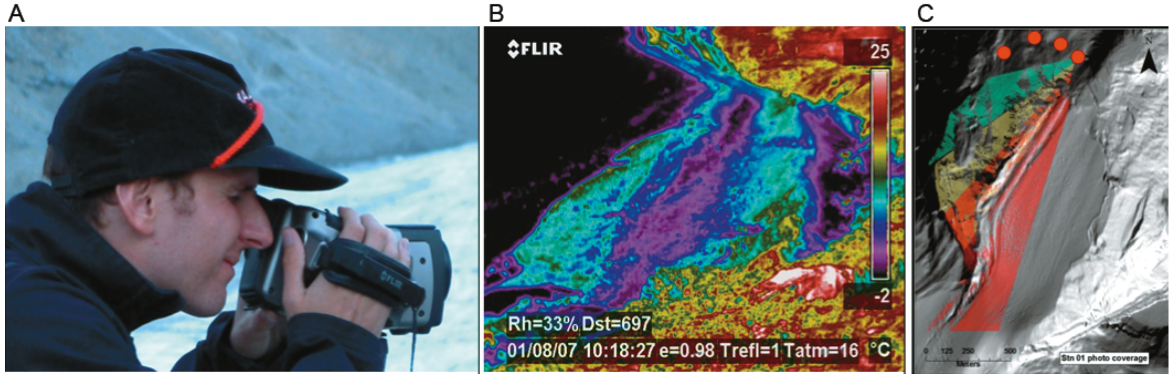

Figure 2. (A) Thermal camera FLIR P being used at Peyto Glacier. (B) TIR image of the glacier medial moraines. Dst, mean distance; *e*, emissivity; Rh, relative humidity; Trefl, estimated surface temperature; Tatm, atmospheric temperature. (C) GPS-located imaging stations (red dots) and individual image viewsheds from station 1.

corrected to the survey monument that was used to control the lidar surveys. Consequently, the photo-stations are accurately positioned relative to the lidar DEM to within a few centimetres, or well within the grid node resolution of the DEM.

After thermal data collection, the images went through several stages of processing so that they could be integrated with the high-resolution three-dimensional (3D) surface data of the lidar DEM and compared through time. The stages are summarized as follows: (*i*) remapping of digital number (DN) values to a linear grey scale, (*ii*) oblique image orthorectification, (*iii*) remapping DN values to original temperature scale, (*iv*) generation of image mosaics for each photo-station and collection period, (*v*) pixel buffering to fill small gaps in coverage, and (*vi*) generation of thermal signatures over glacial and periglacial sites of interest.

The images were orthorectified using the IDL Geophotoref tool developed and described by Corripio (2004). Orthorectification was accomplished by transforming the pixels of the image from the camera coordinate system into that of the 1 m lidar DEM (Corripio, 2004). This required accurate DEM coverage of the entire photograph scene, a viewshed (visible land surface) of the area from the point where the photograph was taken, an 8 bit red–green–blue (RGB) digital image, the camera specifications, and a series of ground-control points that were recognizable on both the photograph and the DEM. A viewshed from each photo-station was needed to ascertain which terrain surfaces were observable and which were occluded within each oblique TIR image. This was produced from the DEM within Geophotoref using the surveyed coordinates of the camera positions. Initial image processing required the addition of two identical bands to satisfy the 8 bit RGB image requirement within the Geophotoref software. Given the manufacturer-quoted thermal accuracy of $\pm 2\,^{\circ}$C, the loss of spectral resolution in converting the image from a 32 bit format to an 8 bit format did not result in any meaningful loss of information. Camera specifications of focal length, photograph centre point, and camera tilt were entered using an iterative approach until the ground-control points on the DEM matched those on the digital photograph. The result of this orthorectification process was a set of temperature pixels distributed across the surface of the DEM as visible from the perspective of the camera. Consequently, each image contained many temperature data gaps due to occlusion from intervening surface obstructions.

Following the orthorectification process, images acquired within the same approximate time frame were collated and mosaiced in ArcGIS 9.3 (ESRI, Redlands, Calif.). In areas of overlapping images, corresponding pixel DN values were averaged to mitigate against abrupt changes in surface temperature along the image edges. In practice, the relatively short time delay between first and last image introduced very little actual surface temperature variation. Even following the mosaic process, the 1 m resolution thermal mosaics still contained data gaps between pixels due to either physical occlusion or an artifact of the pixel remapping process. Consequently, this limited the ability to compare temperature patterns through time using direct raster-to-raster grid comparison techniques in ArcGIS. To overcome this limitation, a region growing buffer was applied to all four mosaics to fill any data gaps up to a maximum distance of 5 m using bilinear interpolation. A limit of 5 m was applied to prevent interpolating pixel temperatures across unrealistically large distances. The resultant thermal image mosaics still possessed data gaps but only in areas of occlusion due to large features in the landscape such as moraine ridges.

Lastly, three approaches were adopted to compare the spatially registered thermal image data through time. The first was to perform raster grid subtractions between adjacent time intervals to visualize the spatial patterns in either increasing or decreasing surface temperatures. The second was to run profiles across the range of glacial moraine land covers of interest and extract the surface temperature signals along the profiles for each time period. The third was to identify points that were known or suspected, based on field evidence, to have different geomorphic properties, and then to extract the thermal signatures of a cluster of points (nine in total) at each of these locations and compare the temperatures through time. The four strata chosen were (*i*) clean glacial ice with virtually no debris cover; (*ii*) medial moraine that is known to possess a thin veneer of debris cover (up to several decimetres) and is internally comprised predominantly of glacial ice; (*iii*) an area of highly mobile moraine identified in Hopkinson and Demuth (2006) and Hopkinson et al. (2009) in which, although there is no ice core visible at the surface, the authors suspect the presence of ice core due to the rapid motion and volumetric loss in the immediate vicinity; and (*iv*) an area of more "stable" moraine where rapid motion and downwasting are not evident, and thus it is assumed to be an area less likely to contain a shallow ice core that could modify surface temperatures. These four sites could not be located immediately adjacent to one another but are within 600 m and generally encounter the same meteorological conditions. To check that the potential for surface heating at each of these sites was approximately equivalent during the experiment, we simulated clear sky diurnal shortwave energy inputs at the DEM surface locations of the four sites.

Results and discussion

The temporal sequence of processed, orthorectified, mosaiced, and buffered oblique thermal images collected over Peyto Glacier on 1 August 2007 is illustrated in **Figure 3**. The spatial variation in daytime temperature increases and nighttime cooling over moraine, ice, and bedrock areas is illustrated. A detailed and accurate interpretation of the observed spatiotemporal variability in temperature signatures requires information of the true land surface emissivity and an analysis of the energy balance inputs to these surfaces throughout the day. Such analysis was outside the scope of this preliminary assessment, but many useful findings can be reported.

Although the actual temperatures over the moraine were not validated, we can draw some preliminary conclusions from the generated thermal image mosaics. Notably, the spatial correspondence in thermal data from image to image during the mosaicing process was high within the area of interest, with maximum temperature differences of 3 °C due to slight misalignments and (or) rapidly changing surface temperature conditions during the course of image collection. By averaging the thermal data in overlap areas, the largest errors have been mitigated and kept within the manufacturer-quoted accuracy of 2 °C. Another encouraging observation is that all clean ice temperatures recorded were between −1 °C and +1 °C. The ice surface was actively melting during the day, and nighttime air temperatures at the research hut did not fall below 0 °C. Therefore, the actual ice temperature is likely to have been 0 °C throughout the data collection. This suggests that, without any postprocessed calibration, the orthorectified thermal image mosaics provide a reasonably accurate map of glacial and moraine surface temperatures.

Although this study was focused on developing a procedure for studying and monitoring the moraine thermal properties rather than actually interpreting and explaining these preliminary results, some qualitative observations can be made that do appear to suggest evidence of heat loss to ice-cored moraine. **Figure 4** illustrates the results of the temporal thermal signature analyses. **Figure 4A** demonstrates that the site and profile data presented in **Figures 4B, 4C, and 4D** were collected over areas receiving similar shortwave energy inputs during the day. There was a shift in the peak of solar insolation from 12:00 at the stable and active moraine areas to 13:00 at the medial moraine and glacial ice areas, but the total receipt of solar energy varied by less than 10% across all sites. Of note, the 16:30 image collection occurred just prior to loss of direct beam radiation over the study area, and the 20:30 collection occurred at sunset, with 22:00 being in complete darkness. Thus, 20:30 to 22:00 was the only time period sampled with no input of solar heating, and this is evidenced by the almost universal drop in surface temperatures over moraine, talus, and bedrock areas in **Figure 4B**. As would be expected, little to no temperature variation occurs over the clean glacial ice surface, and the highest rates of cooling (up to and exceeding 15 °C) occur over the most mobile areas of moraine where ice core is suspected.

Although variations in slope, aspect, shadowing, and micrometeorological conditions influence surface temperatures at the pixel scale, the temperature signatures across surface profiles (**Figure 4C**) and at distinct points of interest (**Figure 4D**) suggest that the moraine and glacial ice strata have distinct thermal properties. In **Figure 4C**, the highest daytime and nighttime surface temperatures are recorded, as is the lowest daytime temperature range, over the stable moraine area. Warmer surface temperatures with reduced temperature variation suggest some thermal stability and support the hypothesis that heat is not being scavenged from this surface to drive internal melt processes. At the opposite extreme, we see glacial ice and medial moraine displaying the lowest temperatures throughout the day, due to most of the energy inputs to these surfaces going into latent heat of melt. The active moraine area lies intermediate to these two zones along the profile in **Figure 4C** and, apart from 10:30 when this area was receiving the greatest input of shortwave radiation (**Figure 4A**), the surface temperatures also lie between the two extremes. Moreover, although the nighttime heat loss between 20:30 and 22:00 is large, the greatest loss of heat appears to closely follow the cessation of direct beam radiation input after 16:30, indicating a rapid loss of stored sensible heat energy.

The diurnal patterns of heating and cooling over the four sites chosen based on a priori knowledge of the surface type are more easily interpreted. In **Figure 4D** we see a gradual progression from higher to lower daytime surface temperatures for stable moraine to active moraine to medial moraine to clean glacial ice. The stable moraine site follows a diurnal heating regime that follows the pattern of solar insolation with a maximum surface temperature exceeding 20 °C.

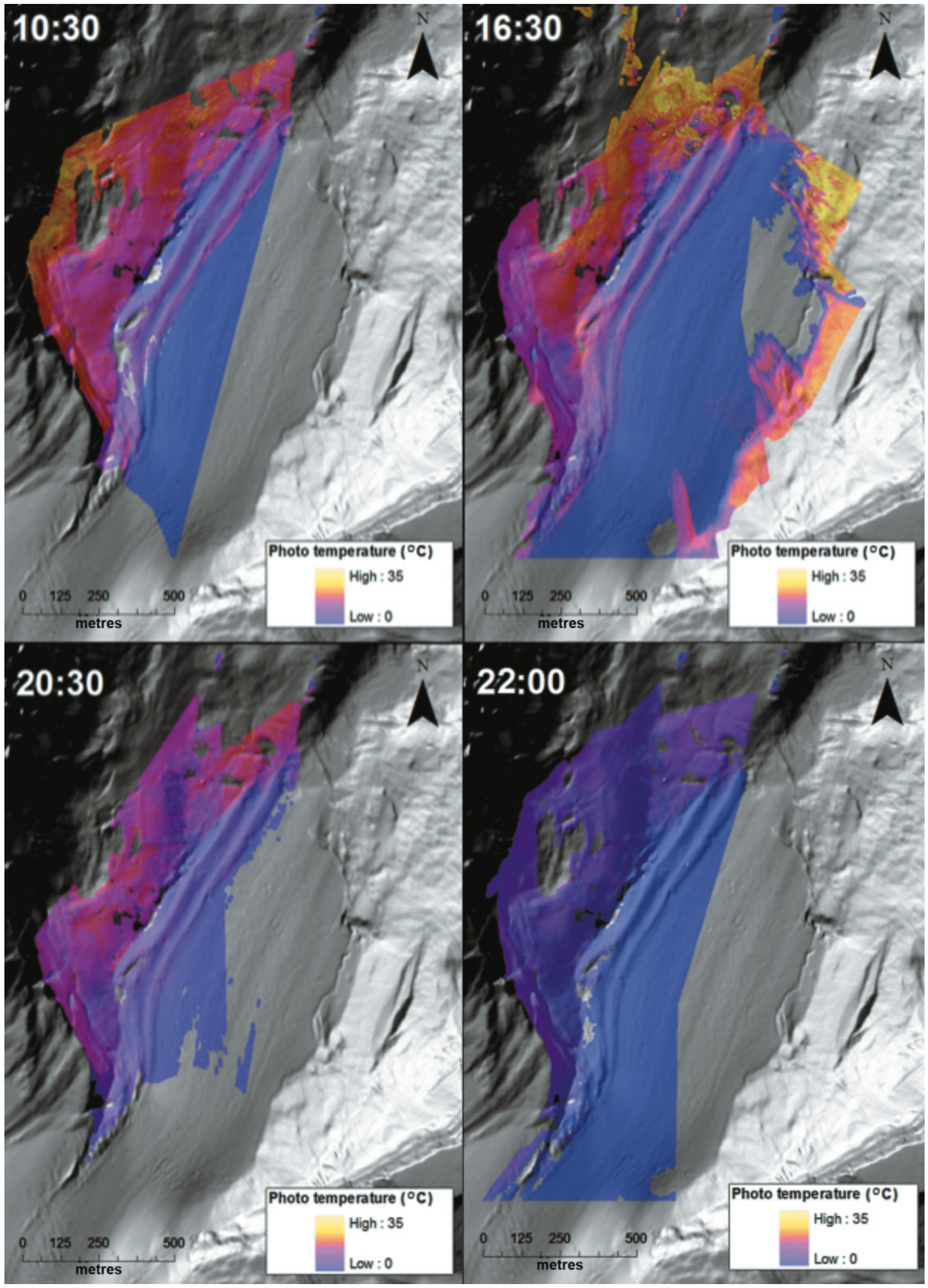

Figure 3. Orthorectified diurnal oblique thermal imagery over medial and lateral moraines at Peyto Glacier, draped over a temporally coincident lidar shaded relief image collected at four different observation times on 1 August 2007.

Active moraine displays lower temperatures and a more rapid loss of heat late in the day. The ice surface behaves as expected, and there is no significant change in temperature from 0 °C throughout the day. Perhaps the most compelling evidence of ice core within the active moraine is that by 22:00 the surface temperature is hovering just above 0 °C. It is also interesting to note that of the signatures presented, that which most closely matches the active moraine site is the medial moraine, which is known to contain a large proportion of shallow ice core.

These observations suggest that time sequences of orthorectified field-collected oblique thermal imagery have the potential to map melt-driven thermal variations in areas of relatively shallow ice-cored moraine. In the nighttime cooling illustrated in **Figure 4B**, it appears that the highest rate of cooling occurs over the areas of moraine that have undergone the most long-term downwasting from 1949 to 2007 and, from recent lidar data, have been identified as the area of highest moraine mobility >6 m/year (Hopkinson et al., 2009). Without explicitly controlling for the spatial variation

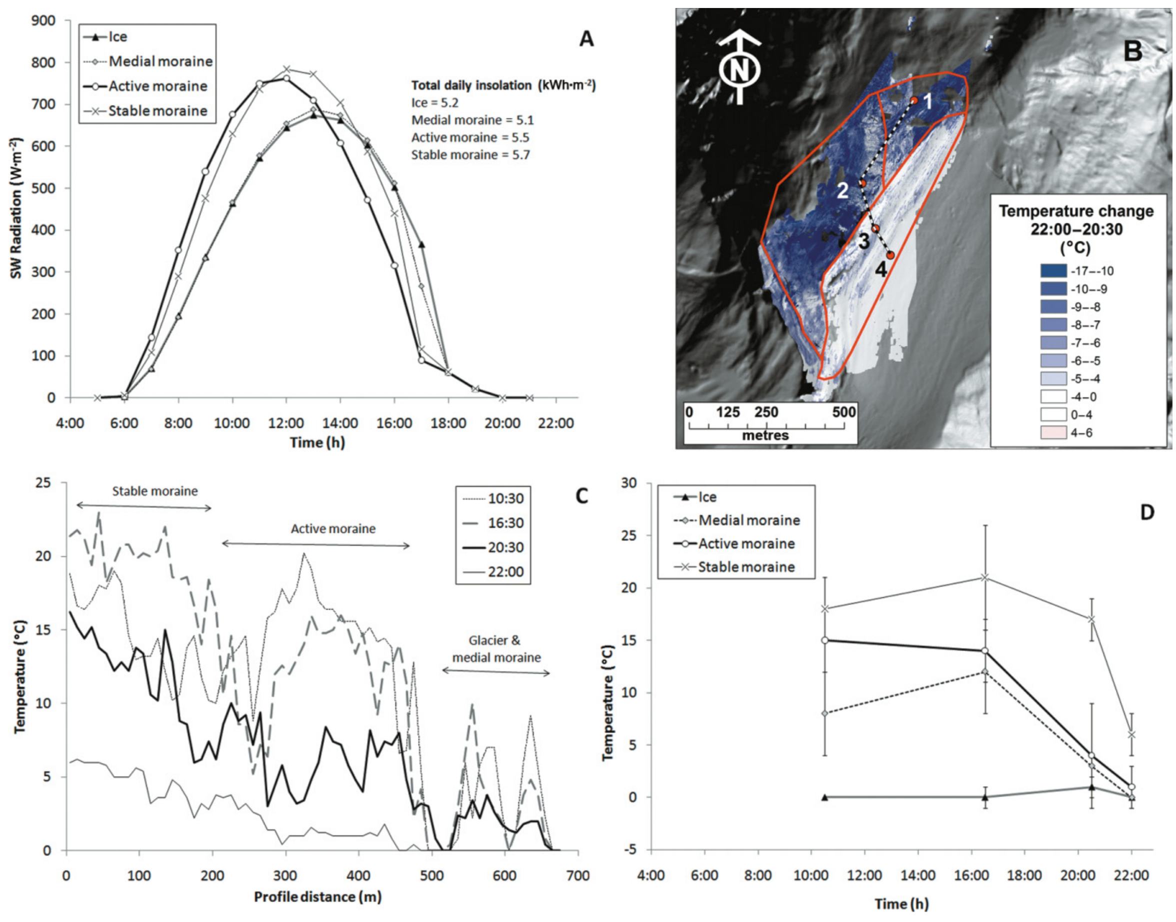

Figure 4. (A) Incoming diurnal solar radiation (SW, shortwave) at four sites characterizing the glacial and moraine land cover types of interest. (B) Thermal change detection image illustrating nighttime cooling patterns over the moraine surfaces. Locations of the four sites and a temperature sample profile are also shown. (C) Diurnal surface temperature profiles (1–2–3–4) taken from the site-to-site profile across the TIR images. (D) Diurnal temperature signals and standard deviation bars for groups of nine pixels representing each of the four surface type sites.

of radiant intensity and turbulent heat fluxes across these surfaces, little can be concluded with certainty, but the data presented from this preliminary methodological study are at least suggestive that ice core within the active or highly mobile moraine area is scavenging heat to drive melt processes throughout the day and into the early evening.

Conclusions

By combining diurnal oblique thermal image sequences with coincident high-resolution light detection and ranging (lidar) data, it was possible to map the spatial variation of surface heating and cooling over the glacial and periglacial surfaces of Peyto Glacier, Canadian Rocky Mountains. As expected, the temperature remained constant over an actively melting glacier ice surface. Some heating was observed over partially debris covered medial moraines, but it was qualitatively apparent that most of the incoming heat was being scavenged to drive the melting of ice immediately beneath the surface. The thermal infrared (TIR) image results over active mobile lateral moraines on the northwest side of the glacier terminus were less obvious to interpret, and it was impossible to derive firm conclusions without either controlling for or monitoring the energy inputs to the surfaces being investigated. By analogue, however, it was apparent that bedrock, talus, and older more stable areas of moraine adjacent to active moraine surfaces were able to heat up at a faster rate and cool down at a slower rate, thus providing a qualitative indicator that ice within the moraines may be scavenging surface heat to drive internal melt processes.

The application of lidar and in situ oblique thermal imaging at Peyto Glacier is being researched for applicability to ongoing glacial monitoring and integration with mass balance and hydrometeorological data collection activities. One concept that is being investigated is the seasonal deployment of a thermal imaging camera programmed to acquire images at predetermined times to capture both diurnal and seasonal variations in surface heat signatures. Targets could be set up both to aid in the georegistration of the TIR imagery but also to allow tracking of moraine surface mobility. Of immediate interest here due to the implication for long-term regional water resources is a better understanding and quantification of the volumes of ice core and depths of moraine debris cover within the periglacial environment. However, by monitoring the surface heat fluxes in this manner we can also integrate automatic weather station (AWS) data to scale up and extrapolate the radiant and turbulent heat transfers within the glacial environment.

The information derived from the integration of lidar and easily acquired in situ thermal imagery has the potential to improve our understanding of melt-driven geomorphic periglacial processes within alpine headwater locations.

Acknowledgments

The studies summarized in this paper are the results of an academic and federal government research and monitoring partnership between the Glaciology Section, Geological Survey of Canada (GSC), and the Applied Geomatics Research Group, Nova Scotia Community College. The lidar data collection activities have been supported and coordinated by the Canadian Consortium for Lidar Environmental Applications Research (C-CLEAR). Funding has been derived from a variety of sources (Meteorological Service of Canada Cryosphere System (CRYSYS), Canadian Foundation for Climate and Atmospheric Sciences (CFCAS), Canadian Space Agency (CSA) Government Related Initiatives Program (GRIP), Canada Foundation for Innovation (CFI), and Natural Sciences and Engineering Research Council of Canada (NSERC)). Several groups and individuals have also provided invaluable assistance at times, in particular, Optech Incorporated (Toronto, Ont.), Mike Sitar, Laura Chasmer, Grace Gillis, and Steve Bertollo. GSC Earth Sciences Sector (ESS) contribution No. 20090306. In part supported by a grant to Mike Demuth from the Canadian Space Agency GRIP.

References

Comeau, L.E.L., Pietroniro, A., and Demuth, M.N. 2009. Glacier contribution to the North and South Saskatchewan Rivers. *Hydrological Processes*, Vol. 23, No. 18, pp. 2640–2653. doi:10.1002/hyp.7409.

Corripio, J.G. 2004. Snow surface albedo estimation using terrestrial photography. *International Journal of Remote Sensing*, Vol. 25, pp. 5705–5729.

Demuth, M.N., and Keller, R. 2006. An assessment of the mass balance of Peyto Glacier (1966–1995) and its relation to recent and past-century climatic variability. In *Peyto Glacier — one century of science*. Edited by M.N. Demuth, D.S. Munro, and G.J. Young. National Hydrology Research Institute (NHRI), Saskatoon, Sask. NHRI Science Report 8, pp. 83–132.

Demuth, M.N., and Pietroniro, A. 1999. Inferring glacier mass balance using RADARsat: results from Peyto Glacier, Canada. *Geografiska Annaler*, Vol. 81A, pp. 521–540. doi:10.1111/j.0435-3676.1999.00081.x.

Demuth, M.N., Munro, D.S., and Young, G.J. (Editors). 2006. *Peyto Glacier — one century of science*. National Hydrology Research Institute (NHRI), Saskatoon, Sask. NHRI Science Report 8. 278 pp.

Demuth, M.N., Pinard, V., Pietroniro, A., Luckman, B.H., Hopkinson, C., Dornes, P., and Comeau, L. 2008. Recent and past-century variations in the glacier resources of the Canadian Rocky Mountains – Nelson River system. *Terra Glacialis*, Vol. 11, pp. 27–52.

Hopkinson, C., and Demuth, M.N. 2006. Using airborne lidar to assess the influence of glacier downwasting on water resources in the Canadian Rocky Mountains. *Canadian Journal of Remote Sensing*, Vol. 32, No. 2, pp. 212–222.

Hopkinson, C., and Young, G.J. 1998. The effect of glacier wastage on the flow of the Bow River. *Hydrological Processes*, Vol. 12, pp. 1745–1763. doi:10.1002/(SICI)1099-1085(199808/09)12:10/11<1745::AID-HYP692>3.0.CO;2-S.

Hopkinson, C., Demuth, M.N., Sitar, M., and Chasmer, L. 2001. Applications of lidar mapping in a glacierised mountainous terrain. In *IGARSS'01: Proceedings of the International Geoscience and Remote Sensing Symposium*, 9–14 July 2001, Sydney, Australia. Edited by T.I. Stein. CD-ROM. IEEE, Piscataway, N.J.

Hopkinson, C., Sitar, M., Barlow, J., Demuth, M.N., Young, G.J., Pomeroy, J., and Munro, D.S. 2009. Investigating glacier dynamics using temporal air photo, lidar and oblique thermal imagery at Peyto Glacier: an overview. In *Proceedings of the 30th Canadian Remote Sensing Symposium*, 22–26 June 2009, Lethbridge, Alta. Canadian Aeronautics and Space Institute (CASI), Ottawa, Ont. Proceeding Number 488.

Johnson, P.G., and Power, J.M. 1985. Flood and landslide events, Peyto Glacier terminus, Alberta, Canada, 11–14 July 1983. *Journal of Glaciology*, Vol. 31, pp. 86–91.

Kääb, A. 2008. Remote sensing of permafrost-related problems and hazards. *Permafrost and Periglacial Processes*, Vol. 19, pp. 107–136.

Krüger, J., and Kjær, K. 2000. De-icing progression of ice-cored moraines in a humid, subpolar climate, Kötlujökull, Iceland. *The Holocene*, Vol. 10, pp. 737–747. doi: 10.1191/ 09596830094980.

Lougeay, R. 1974. Detection of buried glacial and ground ice with thermal infrared remote sensing. In *Advanced concepts and techniques in the study of snow and ice resources*. Edited by H.S. Santeford and J.L. Smith. National Academy of Sciences, Washington, D.C. pp. 487–494.

Lougeay, R. 1982. Landsat thermal imaging of alpine regions. *Photogrammetric Engineering & Remote Sensing*, Vol. 48, pp. 269–273.

Munro, D.S. 2006. Linking the weather to glacier hydrology and mass balance at Peyto Glacier. In *Peyto Glacier — one century of science*. Edited by M.N. Demuth, D.S. Munro, and G.J. Young. National Hydrology Research Institute (NHRI), Saskatoon, Sask. NHRI Science Report 8, pp. 135–176.

Nakawo, M., and Young, G.J. 1982. Estimate of glacier ablation under a debris layer from surface temperature and meteorological variables. *Journal of Glaciology*, Vol. 28, No. 98, pp. 29–34.

Østrem, G., and Arnold, K. 1970. Ice-cored moraines in southern British Columbia and Alberta.*Geografiska Annaler*, Vol. 52A, pp. 120–128. doi:10.2307/520605.

Østrem, G. 1959. Ice melting under a thin layer of moraine and the existence of ice-cores in moraine ridges. *Geografiska Annaler*, Vol. 41, pp. 228–230.

Pomeroy, J.W., Marks, D., Link, T., Ellis, C., Hardy, J., Rowlands, A., and Granger, R. 2009. The impact of coniferous forest temperature on incoming longwave radiation to melting snow. *Hydrological Processes*, Vol. 23, pp. 2513–2525. doi:10.1002/hyp.7325.

Stahl, K., Moore, R.D., Shea, J.M., Hutchinson, D., and Cannon, A.J. 2008. Coupled modelling of glacier and streamflow response to future climate scenarios. *Water Resources Research*, Vol. 44, W02422. doi:10.1029/2007WR005956.

Young, G.J. 1991. Hydrological interactions in the Mistaya basin, Alberta, Canada. In *Snow, hydrology, and forests in high alpine areas*. Edited by H. Bergmann, H. Lang, W. Frey, D. Issler, and B. Salm. IAHS Press, Wallingford, UK. IAHS Publication 205, pp. 237–244.